Prediction the Equivalent Fracture Network Permeability Using Multivariable Regression Analysis and Artificial Neural Networks

Jafari, A. and Babadagli, T.

University of Alberta, Edmonton, Alberta, Canada

tayfun@ualberta.ca

ABSTRACT

Two major steps in the preparation of static reservoir models in naturally fractured reservoirs are fracture network mapping and "upscaling" (converting) the discrete fracture network and its properties, especially permeability, into the parameters which are essential to run reservoir flow simulators. This study presents a new, practical approach to estimate the equivalent fracture network permeability (EFNP) using two different methods (i.e. multivariable regression analysis (MRA) and artificial neural networks (ANN)). Different statistical and fractal characteristics of twenty natural fracture patterns collected from the outcrops of geothermal reservoirs were measured. They were then correlated to the EFNP using MRA and several empirical equations with different values of variables proposed. Next, synthetic fracture networks were generated based on different combinations of fracture length, density and orientation, and their different statistical and fractal characteristics were measured. The EFNPs of these synthetic fracture networks were predicted, using the derived equations to validate the equations. The actual EFNPs in all of these exercises were obtained using a commercial discrete fracture network modeling simulator.

As a final effort, the capability of ANN to improve the correlations obtained through the MRA was exploited. It was shown that a back propagation (BPP) network is capable of being used as a predictive tool to predict EFNP properly.

1. INTRODUCTION

Being located in tectonically active areas, natural fractures in most geothermal reservoirs fully control the fluid flow due to their high permeability compared to the rock matrix (Murphy et al., 2004). Despite remarkable efforts to characterize fractured reservoirs properly and to simulate their performance, modeling of such systems is still considered to be a difficult task due to complex fracture network geometry. This complexity prevents the direct input of this fracture geometry into reservoir simulators (Bourbiaux et al. 1998, 1999).

One modeling approach of naturally fractured reservoirs is the dual-porosity/dual-permeability model (Barenblatt and Zheltov, 1960; Barenblatt et al., 1960; Warren and Root, 1963). An alternative to this is the single porosity model where fractures can be considered as an equivalent medium within each grid cell of the numerical model. In a typical dimension of a reservoir simulator cell, fractures act as an equivalent medium and a permeability tensor can describe their flow properties. This is also the approach used in the technique known as discrete fracture network models (DFN). The difficulty with this methodology is the practical determination of equivalent fracture permeability.

Several methods have been introduced to calculate equivalent fracture network permeability (EFNP). Long et al. (1985) and Cacas et al. (1990) developed 3D fracture flow models, and Massonnate and Manisse (1994) introduced a 3D fracture flow model that takes the matrix permeability into account. Lough et al. (1996) developed a 2D fracture flow model taking the contribution of 3D matrix flows into account. Odling (1992) introduced a 2D model considering the matrix permeability. Later, Bourbiaux et al. (1998) proposed a method to calculate the equivalent permeability by applying a pressure drop between the two sides of the parallelepiped network with a specific boundary condition. Using their model, the equivalent permeability for incompressible steady-state flow through the actual 3D fracture network can be calculated. Each of these methods introduced a new fracture network discretization and utilized numerical techniques that may require heavy computational efforts.

In this study, another method is proposed to calculate the EFNP and facilitate the preparation of static models. The method is based on using the statistical and fractal properties of the fracture networks. It has been shown that natural fracture patterns exhibit fractal characteristics (Barton and Larsen, 1985; La Pointe, 1988; Barton and Hseih, 1989). The fractal properties of a fracture network have some implications on its conductivity (La Pointe, 1988). Generally speaking, fracture connectivity, length, density, aperture, and orientation are the crucial parameters of each fracture network, which control the permeability of that network. For instance, a perpendicular direction of fractures relative to the fluid flow direction might have negative effect on fracture network permeability (Babadagli, 2001). However, the connectivity of a fracture network increases as its fracture length and density increase, (Rossen et al., 2000), and the permeability of the network increases with an increase in its fracture aperture and density (Zhang et al., 1996).

In this study, we first showed the relationship between the statistical and fractal properties of 2-D fracture networks and their EFNP. Then, different empirical correlations with a different number of variables were proposed and tested for natural fracture network patterns observed in the outcrops of geothermal reservoirs. In these exercises, the MRA and ANN approaches were used. The correlations introduced can be used in practical applications to estimate the EFNP for each grid block for input into conventional numerical simulators. The main advantage of this approach is its practicality. Also, all possible fracture network characteristics and their different

statistical/fractal characteristics were considered in this analysis to represent the complexity of fracture networks.

2. DERIVATION OF THE EMPIRICAL EQUATION

20 different 2-D natural fracture patterns were selected representing characteristic fracture networks. 10 of them were collected from different sources in the literature, and a great portion of them were from the outcrops of geothermal reservoirs. The sources used for each of these 10 patterns are given in Table 1. The other 10 patterns were acquired from outcrops of the producing formations in the Kizildere, Germencik, and a few other smaller sized geothermal fields in western Turkey. Some representative patterns are shown in Figure 1(a, b, c and d). Although the images are at meter-scale, they were first digitized in a 100x100m square domain to be consistent with a previous study that used 100x100 m synthetic network patterns (Jafari and Babadagli, 2008). The same process was repeated at the original scale, as explained later. For comparison, representative synthetic fracture patterns are given in Figure 2(a, b and c).
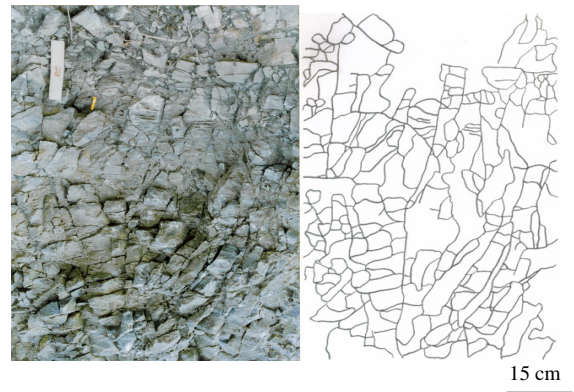
Figure 1 (a, b, c and d). Typical natural (outcrop) fracture patterns from the geothermal fields in western Turkey used in the study.

1a. Outcrop: A producing formation (limestone) in the Kizildere field (photo and fracture trace map).

1b. Outcrop: A producing formation (Limestone) in the Karahayit field (photo and fracture trace map).
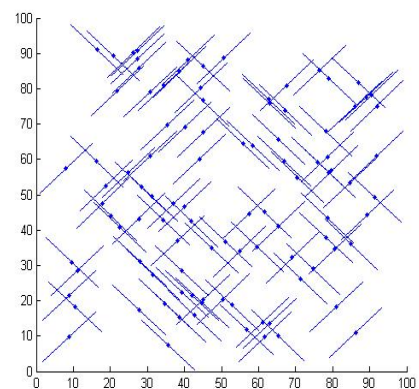

1c. Outcrop: A producing formation (marble) in the Germencik field (photo and fracture trace map).
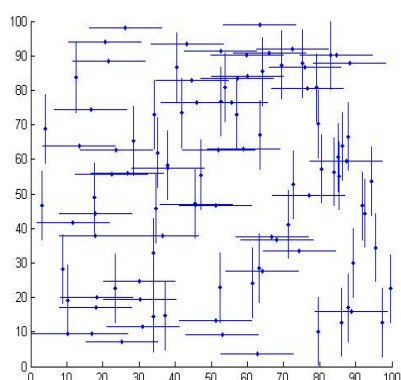

1d. Outcrop: A producing formation (marble) in the Germencik field (photo and fracture trace map).
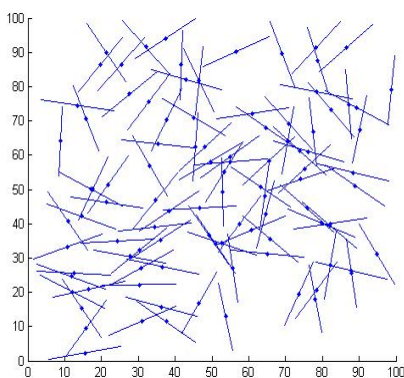
Figure 2 (a, b and c). Typical synthetic model of natural patterns representing different fracture network characteristics (density, length, orientation).

2a. Two fracture sets oriented in NW-SE & NE-SW

2b. Two fracture sets oriented in N-S & E-W

2c. Fractures distributed randomly in all directions.

Table 1. Sources of natural fracture patterns used in the study.

Pattern	Reference
1	Babadagli, 2000
2	Babadagli, 2000
3	Babadagli, 2001
4	Babadagli, 2001
5	Babadagli, 2001
6	Babadagli, 2001
7	Babadagli, 2001
8	Odling, 1992 (A)
9	Odling and Webman, 1991
10	Odling and Webman, 1991

Five statistical and fractal characteristics of the networks were measured, as they showed the highest correlation with the EFNP in a recent study of synthetic networks (Jafari and Babadagli, 2008). These characteristics are given in Table 2. Different features of fracture patterns were considered using different fractal techniques in addition to the statistical parameters shown in the study by Jafari and Babadagli (2008). Using a commercial software package (FRACA), the equivalent permeability tensor of each fracture model with constant conductivity was calculated. In this exercise, only the permeability in the X direction of the equivalent permeability tensor was considered, and the permeability in the Z and Y directions were not taken into account. The EFNPs of the 20 fractal patterns are given in Table 2.

Table 2. Natural fracture patterns in the 100x100 m square domain

FD of Intersection Points using Box Counting Technique	Connectivity Index	Maximum Touch with X Scanning Lines	Maximum Touch with Y Scanning Lines	FD of Fracture Lines using Box Counting Technique	Conductivity mD.m	Permeability mD
1.867	1.064	15608	21143	1.557	1000	28.801
1.820	1.704	15396	17481	1.521	1000	85.936
1.892	1.516	19585	24571	1.598	1000	108.988
1.750	1.407	13331	15887	1.443	1000	56.751
1.774	1.465	15486	16721	1.487	1000	43.032
1.870	1.422	18933	24001	1.576	1000	104.354
1.872	1.275	15916	31323	1.630	1000	106.506
1.800	1.271	13364	16592	1.528	1000	49.509
1.769	1.745	16978	17563	1.567	1000	66.102
1.770	1.496	14366	18920	1.562	1000	70.835
1.298	1.500	489	317	1.270	1000	23.991
1.347	1.100	759	763	1.369	1000	10.387
0.797	1.091	114	266	1.264	1000	38.106
1.672	1.218	4720	5612	1.484	1000	11.863
1.660	1.149	4071	3094	1.493	1000	5.649
1.378	1.020	860	1210	1.481	1000	88.345
1.577	1.041	4697	2680	1.513	1000	9.085
1.893	2.611	4767	5473	1.682	1000	98.342
1.647	1.369	1687	1758	1.583	1000	21.625
1.653	1.558	996	1281	1.515	1000	29.411

FD: Fractal Dimension

Jafari, A. and Babadagli, T.

The first and fifth columns in the table show the fractal dimension (FD) of fracture intersection points and fracture lines, respectively, in the domains using the box counting technique. The second column shows the number of fracture line intersections divided by the number (or density) of fracture lines. The third and forth columns show the results of intersection between fracture lines and imaginary scanning lines in the X and Y directions. The relationship between these parameters and EFNP was investigated using multivariable regression analysis, and three empirical equations were derived with 4, 5 and 6 independent variables, as shown in Table 3.

In Table 3, K represents the permeability (mD). In the first equation, $x1$, $x2$, $x3$ and $x4$ are the fractal dimension of fracture intersection points using the box counting technique, maximum intersection (touch) between fracture lines and the imaginary scanning line in X direction, maximum intersection (touch) between fracture lines and the imaginary scanning line in Y direction, and fractal dimension of fracture lines using the box counting technique, respectively. In the second equation, $x1$, $x2$, $x3$, $x4$ and $x5$ are the fractal dimension of fracture intersection points using the box counting technique, maximum intersection (touch) between fracture lines and the imaginary scanning line in X direction, maximum intersection (touch) between fracture lines and the imaginary scanning line in Y direction, fractal dimension of fracture lines using the box counting technique, and fracture conductivity respectively. In the third equation, $x1$, $x2$, $x3$, $x4$, $x5$ and $x6$ are the fractal dimension of fracture intersection points using the box counting technique, connectivity index, maximum intersection

(touch) between fracture lines and the imaginary scanning line in X direction, maximum intersection (touch) between fracture lines and the imaginary scanning line in Y direction, fractal dimension of fracture lines using the box counting technique, and fracture conductivity, respectively. In all equations, a, b, c, d, e, f, g and h are constant coefficients.

Jafari and Babadagli (2008) proposed an equation to predict the EFNP (the same as the first equation in Table 3, but with different constant coefficients). Initially, this equation was applied to natural fracture patterns. The comparison of the actual and calculated EFNPs is shown in Figure 3. Though the same scale (100x100m) was used, the correlation is not very strong due to the fact that the equation was derived using synthetic (and random) patterns showing topologically different characteristics (poor connectivity, dead end fractures, isolated fractures, etc. exist in synthetic patterns).

Having seen poor correlation with the existing correlation derived by Jafari and Babadagli (2008) using 800 synthetic patterns of different fracture network characteristics (Figure 3), these new equations were generated by MRA using only 20 natural patterns from different geothermal reservoir outcrops.

The comparisons of actual and calculated EFNP values are shown in Figures 4, 5 and 6 for the equations given in Table 3. These plots show the reliability of the equations, and they increase slightly with increasing variables.

Table 3. Derived equations for EFNP (K) with different number of independent variables. Method: MRA.

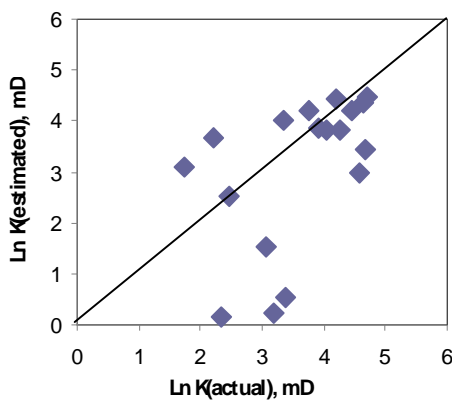| Independent Variables	Derived Equation
4	$Ln(K) = a*exp(b*x1)+c*ln(x2)+d*ln(x3)+ln(x4)+f$
5	$Ln(K) = a*exp(b*x1)+c*ln(x2)+d*ln(x3)+e*ln(x4)+f*ln(x5)+g$
6	$Ln(K) = a*exp(b*x1)+c*ln(x2)+d*ln(x3)+e*ln(x4)+f*ln(x5)+g*ln(x6)+h$

Figure 3. Comparison of actual and estimated EFNPs using the Jafari and Babadagli (2008) equation with 4 independent variables for natural patterns.
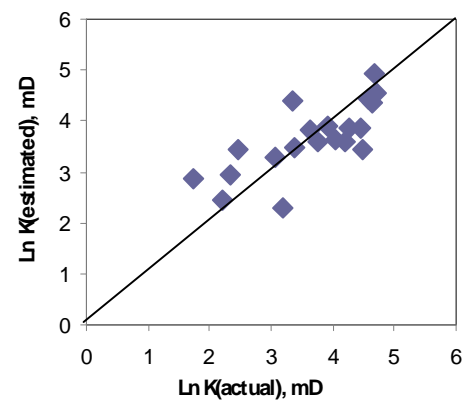

Figure 4. Comparison of actual and estimated EFNPs using the equation with 4 independent variables for natural patterns.
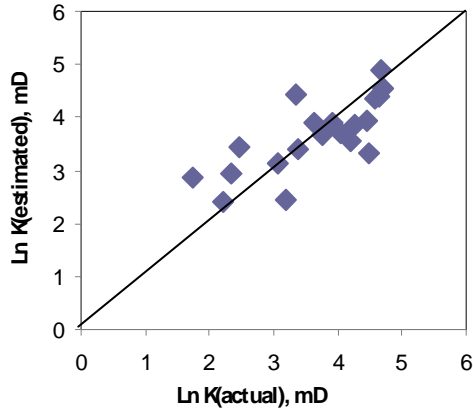
Figure 5. Comparison of actual and estimated EFNPs using the equation with 5 independent variables for natural patterns.
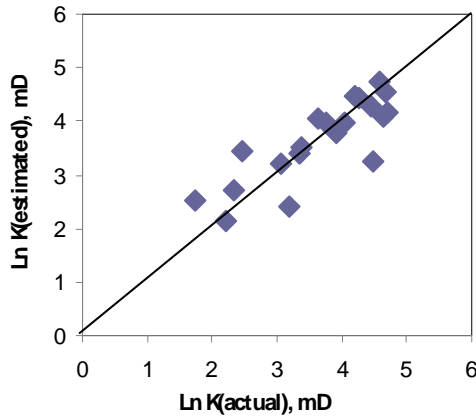

Figure 6. Comparison of actual and estimated EFNPs using the equation with 6 independent variables for natural patterns.

To validate these equations, different synthetic patterns were generated according to the following algorithms. First, synthetic 2D fracture models within 100x100m square domains were generated, typical patterns of which are shown in Figure 2. A wide range of fracture lengths, densities, and orientations were considered in the patterns used for this validation process. In each model, fracture seeds are distributed according to a uniform distribution, and each fracture is represented as a line in the fracture domain. The range of each fracture parameter in this algorithm is as follows:

(1) Fracture length (in m): (a) constant: 20, 40, 60, and 80; (b) variable with a normal distribution and mean values of 20, 40, 60, and 80.

(2) Density (# of fractures/domain): 50, 100, 150, 200 and 250 (domain is 100x100m).

(3) Orientation: Two fracture sets in the domain with the directions of (a) N-S & E-W, (b) NW-SE & NE-SW and (c) totally random.

It should be mentioned that instead of aperture, conductivity was used, which is related to aperture since the product of the intrinsic fracture permeability and the fracture aperture with parallel walls is defined as conductivity (Bourbiaux et al. 1998). Each data set contained twenty different combinations of length and density. Also, five different realizations using different random number seeds for each combination were used to include the effect of randomness. Each of these models could represent one grid cell in dual-porosity simulators. Using the same software, their equivalent fracture permeability was then measured. In order to validate the derived equations, these permeability values were estimated using these equations and plotted against each other for comparison purposes. These comparisons are shown in Figures 7, 8 and 9.
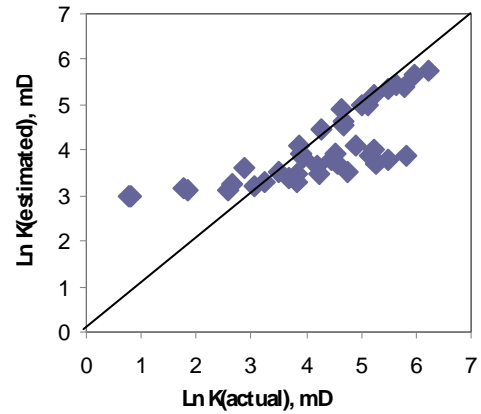

Figure 7. Comparison of actual and estimated EFNPs using the equation with 4 independent variables. Validation of the equation derived for natural patterns using synthetic patterns.
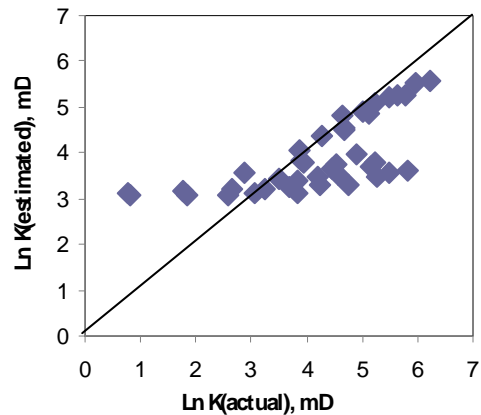

Figure 8. Comparison of actual and estimated EFNPs using the equation with 5 independent variables. Validation of the equation derived for natural patterns using synthetic patterns.
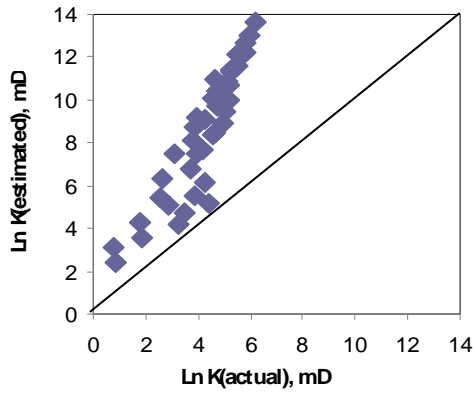
Jafari, A. and Babadagli, T.

Figure 9. Comparison of actual and estimated EFNPs using the equation with 6 independent variables. Validation of the equation derived for natural patterns using synthetic patterns.

The results show that the new equations with 4 and 5 variables derived using natural patterns showed reasonably good correlation for high permeability cases (higher density and longer fractures, i.e., well connectivity). Conversely, the equation with 6 showed significantly higher deviation from the actual values for higher EFNP cases. Obviously, the nature of the synthetic fracture patterns is different from that of natural patterns, and this difference is pronounced clearly in this analysis. For example, the additional parameter used in the 6-variable equation is the connectivity index, and when this parameter is added to the MRA, the correlation becomes much weaker, as can be seen in Figure 9. In fact, the density and length distributions of natural and synthetic (random) patterns can be approximated, as they are statistical parameters, but the connectivity characteristics depend on the nature of the fracturing process and may differ in natural and synthetic patterns. In other words, synthetic and natural fracture patterns may have statistically similar density and fracture length distributions, but connectivity is a topological parameter that has to do with the nature of the fracturing process (and other parameters like lithology), which may not be approximated as a random process. It should also be noted that in generating synthetic patterns, it was assumed that fracture seeds are distributed according to a uniform distribution, which may not always be the case in the field. This directly affects the connectivity rather than density and length, as they are predefined parameters. These observations indicate that one has to pay attention when modeling fracture networks using the discrete fracture network approach or similar techniques to represent the natural patterns, especially when the EFNP is concerned.

The efforts made thus far compared natural and synthetic pattern characteristics by generating 100x100m (typical numerical grid size scale) synthetic patterns and approximating the meter-scale natural patterns to the same size. The next step was to analyze the effect of the domain scale on the correlations and scale the dependency of the EFNP. To achieve this, a much smaller fracture domain was considered (meter-scale) using the same patterns at their original scale. In other words, the same natural patterns were digitized in a 1x1m square domain. Some patterns were larger than 1x1m (at higher scales) and were excluded from this analysis. The same

procedure used for the larger scale was followed to derive new correlations based on the equations in Table 3 (with different coefficients). These equations with new coefficents were tested to predict the EFNPs. The correlations were good for the 4 and 5 variable cases (Figures 10 and 11, respectively), with the exception of two outlying patterns.
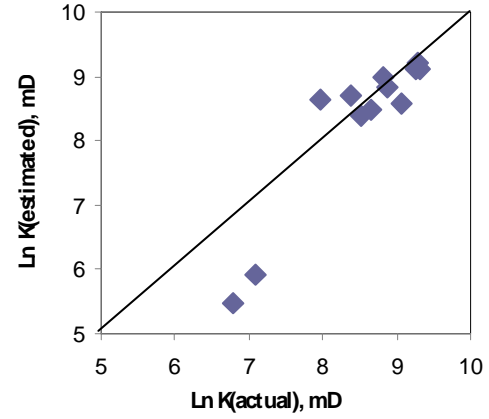

Figure 10. Comparison of actual and estimated EFNPs using the equation with 4 independent variables for 1x1 m square domain. Derived using only natural patterns.
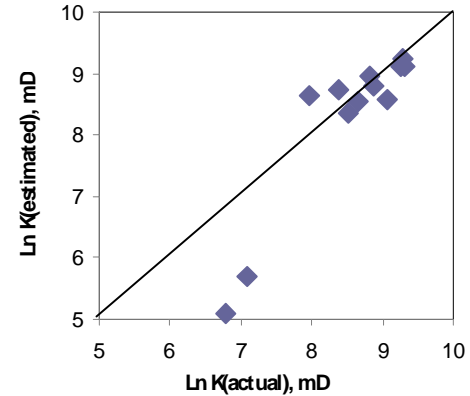

Figure 11. Comparison of actual and estimated EFNPs using the equation with 5 independent variables for 1x1 m square domain. Derived using only natural patterns.

These two patterns belong to a different lithology showing fracture patterns strongly oriented in one direction. When the 6-variable equation is used, one may observe two additional patterns showing deviation, as shown in Figure 12. They belong to much smaller size patterns than 1x1m, but they are stretched to this size while digitizing and placed in a 1x1m domain. Other than these exceptions, the patterns showed reasonably good correlations.

In summary, the equations given in Table 3 are useful to estimate the EFNP of not only the synthetic but also the natural fracture patterns. However, one must pay attention to the scale dependency and use proper coefficients at different scales.
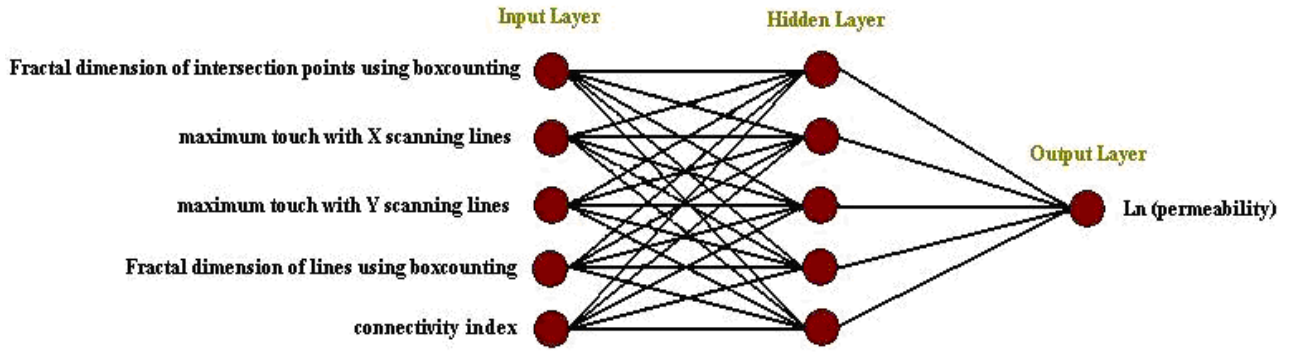
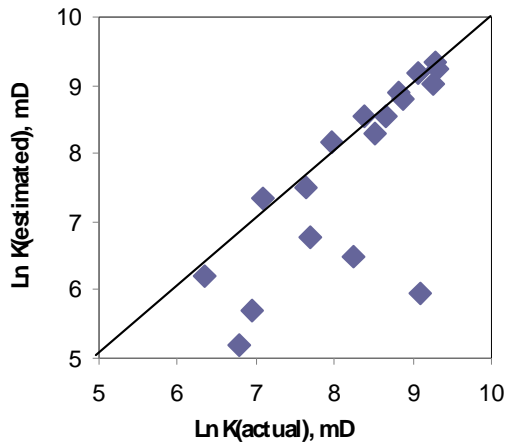**Figure 13. Topology of a back propagation network used in this study.**

Figure 12. Comparison of actual and estimated EFNPs using the equation with 6 independent variables for 1x1 m square domain. Derived using only natural patterns.

4. ARTIFICIAL NEURAL NETWORKS

Improvement of the accuracy of the equivalent fracture network prediction was also attempted. It is believed that the relationships between the EFNP and different fracture network parameters are nonlinear and very complicated; thus, multivariable regression analysis may be limited in capturing these complex relationships. Therefore, an ANN was selected to develop a correlation between the EFNP and fracture network parameters, and the results of this compared to those of the MRA analysis.

A back propagation network was selected to model the problem, and different input variables and numbers in the input layer, different numbers of the hidden layers (between input and output layers), and neurons in each of these hidden layers were tested. In these structures, only one output was defined in the output layer. The structure of the network is shown in Figure 13.

First, all natural fracture pattern data were gathered and divided into three sets: 1) Training set 2) Validation set and 3) Test set. The "Training set" was used to train the network and capture the existing relationship. In the training process, the

inputs and target are given, and the network calculates its error (i.e. the difference between the target and response) and adjusts the weights of the connections between the different neurons. In order to prevent the memorization of the data set by the network, another set called the "Validation set" was input during the training process. Thus, as soon as the error for this set began to increase, the training process stopped. The "Test set" was used to check the ability of the network to predict unseen or new data. The plot of the training, validation and test errors is shown in Figure 14.

Note that in the training process, some synthetic patterns were also used in addition to the natural ones in order to allow extreme values of the EFNP (covering the whole range).

Then, the real equivalent fracture permeability values of all three data sets were plotted against the estimated values by the trained networks. This showed a very promising correlation coefficient, as shown in Figure 15.

Finally, only the input parameters of the synthetic fracture patterns were given to the trained network, and it predicted the equivalent fracture network permeability values. The results are shown in Figure 16. Compared to the cases given in Figures 7, 8 and 9, the reliability of the correlations improved significantly.
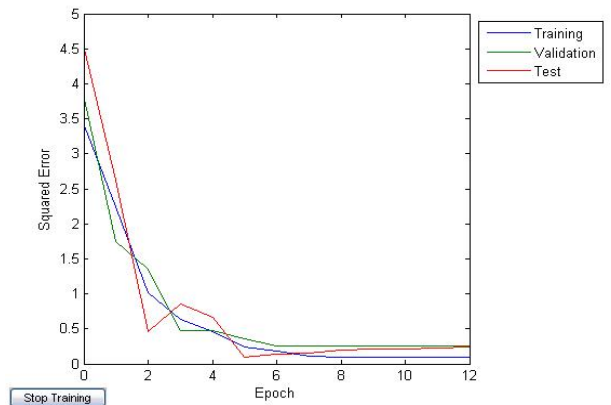

Figure 14. The error of three different data sets (training, validation and test) during the training process.
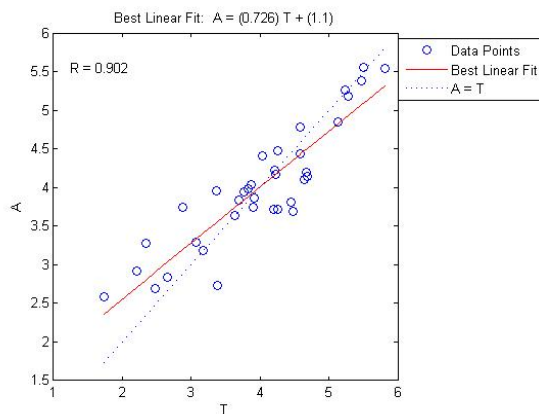
Figure 15. Cross plot comparing actual EFNP of the entire data set (training, validation and testing) to the estimated values. Natural patterns and some synthetic patterns were used for training, validation, and testing.
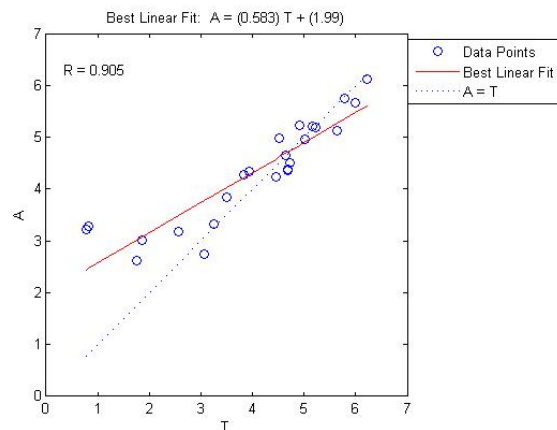

Figure 16. Cross plot showing the comparison of actual and estimated EFNPs of synthetic fracture patterns.

5. CONCLUSIONS

1) The relationship between different statistical and fractal parameters of fracture networks and their equivalent fracture network permeability (EFNP) was studied using natural patterns obtained from geothermal reservoir outcrops. It was shown that the parameters that could be used for the derivation of the empirical equations to predict EFNP are the fractal dimension of fracture intersection points and fracture lines using the box counting technique, connectivity index, the maximum number of intersections between fractures and imaginary scanning lines in the X and Y directions, and conductivity.

2) The equations given in Table 3 are useful to estimate the EFNP of both synthetic and natural fracture patterns. However, one must pay attention to the scale dependency and use proper coefficients at different scales.

3) The connectivity was found to be a critical parameter in the use of synthetic (or random) approaches to model natural fracture networks. The density and length distributions of natural and synthetic (random) patterns can be approximated, as they are statistical parameters, but the connectivity characteristics depend on the nature of the fracturing process and may differ in natural and synthetic patterns. In other words, synthetic and natural fracture patterns may have the same density and fracture length distribution (statistically similar to each other), but connectivity is a topological parameter that is related to the nature of the fracturing process (and other parameters like lithology), which may not be approximated as a random process. These observations indicate that one must pay attention when generating fracture networks using the discrete fracture network approach or similar techniques to represent the natural pattern, especially concerning EFNPs.

4) It was found that a BPP network with one hidden layer containing 5 neurons is capable enough to capture the relationship between the fracture network parameters as inputs and the EFNP as an output. This type of ANN configuration yielded more reliable correlations than the ones obtained with the MRA.

REFERENCES

Babadagli, T., 2001: "Fractal analysis of 2-D fracture networks of geothermal reservoirs in south-western Turkey". J. of Volcanology and Geoth. Res. 112, 83-103.

Babadagli, T., 2000: "Evaluation of outcrop fracture patterns of geothermal reservoirs in southwestern Turkey". Proceedings World Geothermal Congress, Kyushu, Tohoku, Japan, May 28 - June 10.

Barenblatt, G. I., and Zheltov, Y. P., 1960: "Fundamental Equations of filtration of homogenous liquids in fissured rocks". Sov. Dokl. Akad. Nauk., Engl. Transl., 13, 545-548.

Barenblatt, G. I., Zheltov, Y. P. and Kochina, I. K., 1960: "Basic concepts in the theory of seepage of homogenous liquids in fissured rocks". Sov. Appl. Math. Mech., Engl. Transl., 24, 852-864.

Barton, C.C., Larson, E., 1985: "Fractal geometry of two-dimensional fracture networks at Yucca Mountain, south-western Nevada". Proceedings of Int. Sym. on Fundamentals of Rock Joints, Bjorkliden, Sweden. 77-84.

Barton, C. C. and Hsieh, P. A., 1989: "Physical and hydrologic-flow properties of fractures". Field Trip Guidebook, T385, 28th Int. Geol. Cong. Washington DC.

Bourbiaux, B., Cacas, M. C., Sarda, S. and Sabathier, J. C., 1998: "A rapid and efficient methodology to convert fractured reservoir images into a dual-porosity model". Oil & Gas Science and Technology - Rev. IFP, Vol. 53 (1998), No. 6, pp. 785-799, DOI:10.2516/ogst:1998069).

Bourbiaux, B., Granet, S., Landereau, P., Noetinger, B., Sarda, S. and Sabathier, J. C., 1999: "Scaling up matrix-fracture transfers in dual-porosity models: Theory and Application". SPE 56557, Annual Technical Conference and Exhibition held in Houston, Texas, 3–6 October.

Cacas, M. C., Ledoux, E. and De Marsily, G., 1990: "Modeling fracture flow with a stochastic discrete fracture network: Calibration and Validation". Water Resources Research, 26, 3, 479-500.

Jafari, A. and Babadagli, T., 2008: "A Sensitivity Analysis for Effective Parameters on Fracture Network Permeability". SPE 113618, Western Regional and Pacific Section AAPG Joint Meeting, Bakersfield, California, U.S.A., 31 March–2 April 2008.

La Pointe, P. R., 1988: "A method to characterize fracture density and connectivity through fractal geometry". Int. J. Rock Mech. Min. Sci. Geomech. Abstr., 25, 421-429.

Long, J. C. S., Gilmour, P. and Witherspoon, P. A., 1985:"A model for steady fluid flow in random three-dimensional networks of disk-shaped fractures". Water Resources Research, Vol. 21, 8, 1105-1115.

Lough, M. F., Lee, S. H. and Kamath, J., 1996: "A new method to calculate the effective permeability of grid blocks used in the simulation of naturally fractured reservoirs". SPE 36730, SPE Annual, Technical Conference and Exhibition, Denver, Colorado, U.S.A.

Massonnat, G. and Manisse, E., 1994: "Modelisation des reservoirs fractures et recherché de parameters equivalents: etude de l'anisotropie verticale de permeability". Bull. Centres Rech. Explor. Prod. Elf Aquitaine, 18, 171-209.

Murphy, H., Huang, C., Dash, Z., Zyvoloski, G. and White, A., 2004: "Semianalytical solutions for fluid flow in rock joints with pressure-dependent openings". Water Resources Research, Vol. 40, W12506, doi: 10.1029/2004WR003005.

Odling, N.E., 1992: "Permeability of natural and simulated fracture patterns, structural and tectonic modelling and its application to petroleum geology, NPF Special Publication 1, 365-380, Elsevier, Norwegian Petroleum Society (NPF).

Odling, N. E., 1992(A): "Network Properties of a Two-dimensional Natural Fracture Pattern," PAGEOPH, Vol. 138, No. 1, Pages 95-114.

Odling, N. E. and Webman, I., 1991: "A "Conductance" Mesh Approach to the Permeability of Natural and Simulated Fracture Patterns". Water Resources Research, Vol. 27, No. 10, Pages 2633-264.

Rossen, W. R., Gu, Y. and Lake, L. W., 2000: "Connectivity and permeability in fracture networks obeying power-law statistics". SPE 50720, paper presented at the SPE Permian Basin Oil and Gas Rec. Conf., Midland, TX, 21-23 March.

Warren, J. E. and Root, P. J., 1963: "The behavior of naturally fractured reservoirs," SPEJ, September, 245-255.

Zhang, X., Sanderson, D. J., Harkness, R. M. and Last, N. C., 1996: "Evaluation of the 2-D permeability". Int. J. Rock Mech. Min. Sci. Geomech. Abstr. 33 (1), 17-37.